THE ASTROPHYSICAL JOURNAL, 226:172–185, 1978 November 15

HEAVY ELEMENT ABUNDANCES OF NOVA CYGNI 1975

G. J. FERLAND AND G. A. SHIELDS
McDonald Observatory and Department of Astronomy, The University of Texas at Austin
Received 1978 February 16; accepted 1978 May 25

ABSTRACT

McDonald observations of the nebular phase of the outburst of Nova Cygni 1975 are analyzed to measure the abundances of several heavy elements. A new analytical procedure is used to derive the electron density and temperature from the emission line intensities of [O III], [Ne III], and He I observed between days 40 and 120. These physical conditions are used to derive the abundances. We find that Fe has approximately a solar abundance, whereas C, N, O, and Ne are enhanced by factors ~20 to 100. The enhanced abundance of neon was theoretically unexpected.

The derived physical conditions and line intensities are compared with predictions of an equilibrium photoionization model. The model successfully predicts the intensities of He I, [O III], and [Ne III]; but it underestimates the strengths of [Ne V] and [Fe VII], which may originate in a mechanically heated "subcoronal" line region.

Subject headings: stars: abundances — stars: individual — stars: novae

I. INTRODUCTION

Novae have long been suspected of having abnormal heavy-element abundances, because of peculiar spectral line strengths. McLaughlin (1936) identified especially strong carbon and nitrogen absorption lines in spectra of several novae. Nova GK Persei 1901, the first well-studied nova, displayed very strong neon lines during its nebular stage (Payne-Gaposchkin 1957). Spencer-Jones (1931) found that iron lines were remarkably strong during all stages of the 1925 outburst of RR Pic. Unfortunately, the uncertainties in the physical conditions within the ejecta make it difficult to measure abundances reliably.

Historically, chemical abundances have been measured during two stages of the nova outburst. Spectra of many novae appear stellar (broad absorption lines with little or no emission) during the rise to maximum. A curve of growth may be used to convert equivalent widths to column densities if the details of the line formation are understood. However, Williams (1977) found that independent analyses of the absorption lines of a single nova are often inconsistent. Evidently the analysis is extremely sensitive to the values of the microturbulence and temperature assumed, and hence unlikely to give reliable results.

Abundances may also be measured during the nebular stage, when the density is much lower ($N_e \lesssim 10^8$ cm^{-3}) and the spectrum resembles that of a photoionized nebula. Standard nebular techniques (Aller and Liller 1969; Osterbrock 1974) may be used to convert line intensities to abundances if we can estimate the relevant physical conditions. Pottasch (1959) first applied nebular theory to nova ejecta. Collin-Souffrin (1977) reports that the "average" emission study finds that oxygen is enhanced by ~10 relative to the Sun, carbon is enhanced by ~30, Fe may be slightly enhanced, and neon has a solar abundance.

Metal abundances are an important clue to the energy source of the nova outburst. It is generally accepted that novae are close binaries with a late dwarf filling its Roche lobe and transferring material onto a white dwarf. Starrfield *et al.* (1972), Starrfield *et al.* (1974), and Sparks, Starrfield, and Truran (1978) have investigated the conditions necessary to produce an outburst by runaway proton capture onto CNO nuclei in the (accreted) hydrogen-rich envelope of the white dwarf. Slow novae, such as Nova HR Delphini 1967, are the result of outbursts in envelopes with nearly solar abundances. Fast novae, such as V1500 Cygni 1975, occur if the envelope is overabundant in CNO by 50 to 100 times solar. Colvin *et al.* (1977) have suggested that these overabundances could be the result of convective mixing of the envelope with the carbon core of the white dwarf.

Accurate estimates of the mass and chemical composition of nova ejecta are necessary if we are to understand the role of novae in the chemical evolution of our Galaxy. Nova ejecta should be especially rich in ^{13}C, ^{15}N, and ^{17}O since the Starrfield mechanism adds a neutron to the ejected CNO; but Sneden and Lambert (1975) set limits of $^{12}C/^{13}C \geq 1.5$ and $^{14}N/^{15}N \geq 2$ from their analysis of the CN absorption lines in the spectrum of Nova DQ Herculis 1934. Novae may be the dominant contributor to the galactic nucleosynthesis of these isotopes (Audouze, Lequeux, and Vigroux 1975).

The purpose of this paper is to derive the mass and chemical abundances of the ejecta from the very fast galactic nova V1500 Cygni from observations of its emission line spectrum. V1500 Cygni had the most luminous maximum and the most rapid rate of decline of the bright novae of this century (Young *et al.* 1976).

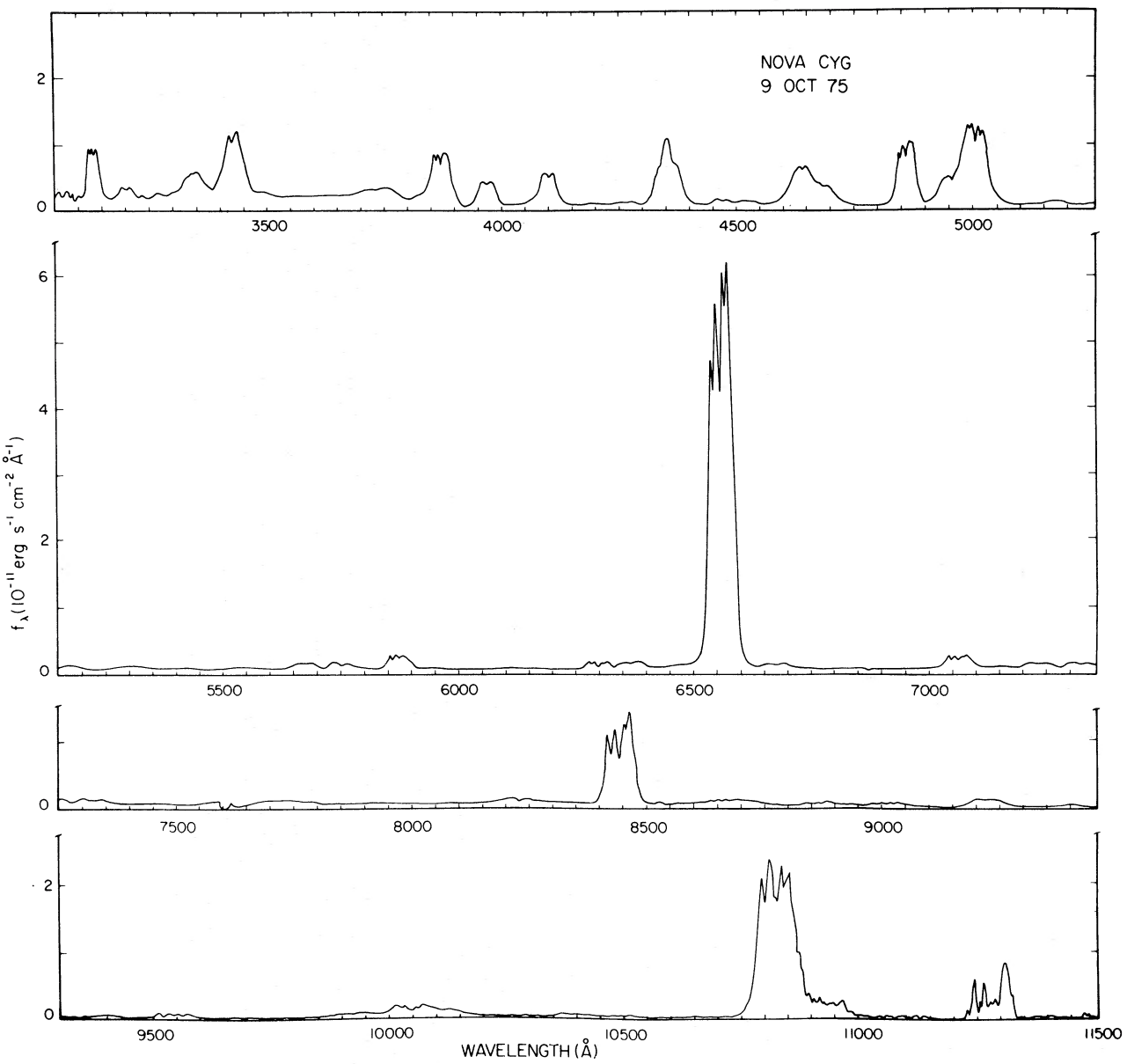

FIG. 1

FIGS. 1–3.—Spectrophotometry of V1500 Cygni. These scans were obtained by Dr. J. Woodman with the single-channel scanner at the coudé focus of the 2.7 m reflector. They are at 4 Å to 8 Å resolution.

Nova Cygni 1975 is an excellent candidate for an abundance study because a large body of photoelectric data exist and because theoretical models predict that the ejecta should be especially overabundant in heavy elements (Starrfield *et al.* 1974).

II. OBSERVATIONS

At the McDonald Observatory, an extensive series of spectrophotometric observations of Nova Cygni 1975 began shortly (1975 Aug. 30.3) after discovery. The data of the first 20 days have been discussed by Tomkin, Woodman, and Lambert (1976). Here we consider data obtained during the late nebular phase, when the nova spectrum resembled that of a planetary nebula or Seyfert galaxy nucleus. A rich display of recombination, collisionally excited, and fluorescent emission lines was present.

We show representative scans in Figures 1–3. These data were obtained 41.8, 78.6, and 120.6 days after outburst (following Ennis *et al.* 1977 we reckon time from t_0 = 1975 Aug. 28.5). The power in individual emission lines was measured by drawing an interpolated continuum beneath the line and measuring the

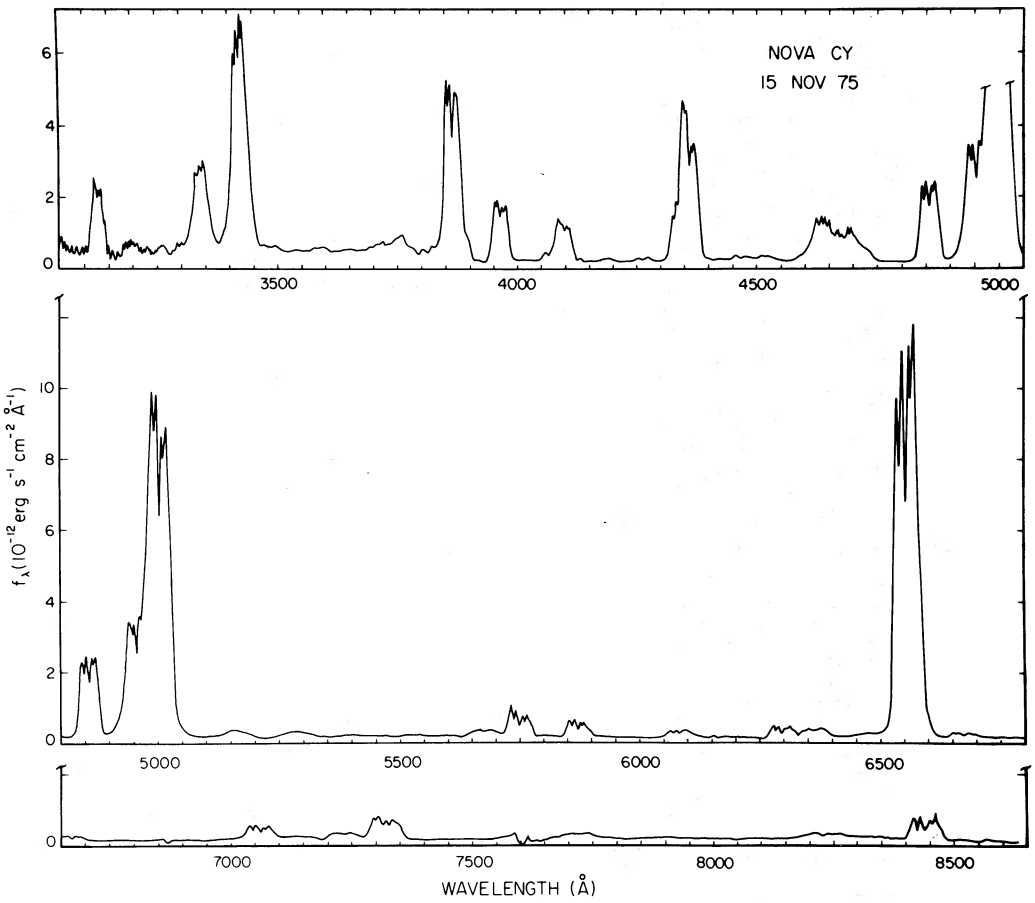

FIG. 2

TABLE 1

EMISSION LINE INTENSITIES

ION	λ	REDDENING-CORRECTED INTENSITY			DAY	OBSERVED INTENSITY		
		42	79	121		42	79	121
Hα	6563	4.45	3.68	3.04		7.50	6.21	5.13
Hβ	4861	1.00	1.00	1.00		1.00	1.00	1.00
Hγ + [O III]	4340 + 4363	1.43	2.52	2.38		1.12	1.99	1.88
He I	5876	0.19	0.15	0.14		0.27	0.21	0.19
He II	5412	0.013	0.019	0.022		0.011	0.015	0.018
C II	4267	0.045	0.053	0.043		0.035	0.041	0.033
C III	4187	0.006	0.03	0.007		0.004	0.02	0.005
[N II]	5755	0.097*	0.25	0.43		0.13*	0.34	0.62
[O I]	6300	0.077	0.11	0.08		0.12	0.17	0.13
[O II]	7325	0.060	0.20	0.39		0.12	0.40	0.78
[O III]	5007, 4959	2.00	6.25	13.03		2.10	6.60	13.73
[Ne III]	3869	1.07	2.87	3.78		0.72	1.93	2.55
[Ne III]	3968	0.48	0.91	1.16		0.34	0.63	0.81
[Ne V]	3426	1.51†	4.37	5.27		0.85†	2.43	2.94
[Fe VII]	6087	0.020	0.079	0.13		0.029	0.12	0.20

* Blended with several [Fe II] lines.

† Blended with O III λ3444.

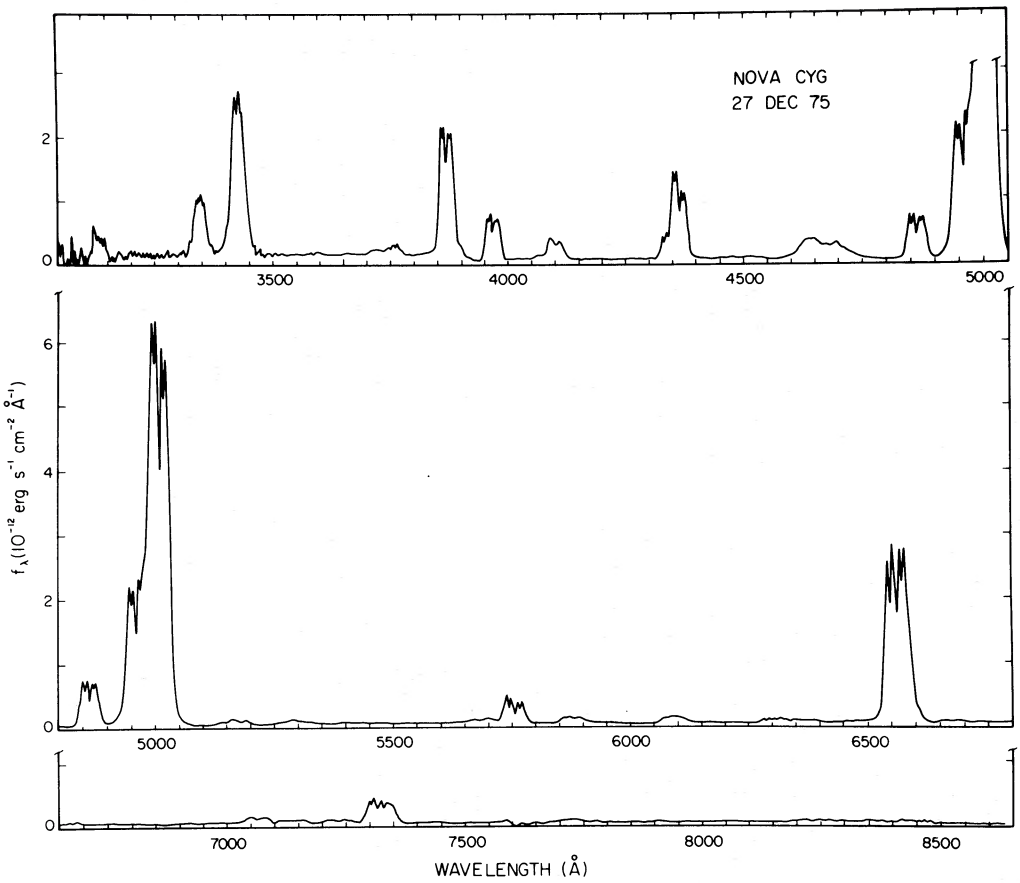

FIG. 3

residual flux. Table 1 gives some line intensities derived from these observations. The observed Hβ fluxes on days (42, 79, 121) were (36.7, 8.6, 2.4) × 10^{-11} ergs s^{-1} cm^{-2}. After correction for reddening of $E(B-V)$ = 0.51, these fluxes give Hβ luminosities at the source of (87, 17.0, 4.6) × 10^{34} ergs s^{-1} for an assumed distance d = 1800 pc.

III. PHYSICAL CONDITIONS

Electron temperatures and densities are required to derive abundances from forbidden emission line intensities. Gallagher and Ney (1976) and Ennis *et al.* (1977) have shown that the nova ejected a thin, possibly irregular, shell at roughly 1975 Aug. 28.5. It resembled the optically thick photosphere of a late B star for several days, then became optically thin in the optical continuum as the column density fell. Forbidden lines of O, Ne, Fe, etc., appeared when the density fell below $N_e \approx 10^9$ cm^{-3}. In this section we use forbidden line strengths to measure the electron density and temperature during the decline. These values will be used in the following section to determine abundances of some heavy elements.

The high density and large Doppler widths of the emission lines preclude our use of the standard emission line ratios to estimate the electron temperature and density. Instead we shall estimate the physical conditions by observing the effects of the declining electron density on certain line ratios: initially the low-lying metastable levels of O^{++} and Ne^{++} were populated as in LTE. As the density fell, various levels were affected differently, allowing us to infer the density and temperature throughout the decline.

a) Reddening

The Balmer decrement of Nova Cygni 1975 deviates from pure recombination in a time-dependent fashion. This can be understood in terms of a variable Balmer line self-absorption and a constant color excess, $E(B-V) = 0.51 \pm 0.05$ (Ferland 1977). In our analysis, we have corrected the emission line intensities for reddening with this color excess and the numerical form of the Whitford (1958) curve presented in Miller and Mathews (1972). Corrected line intensities at various epochs are given in Table 1. In our analysis, we shall adopt an Hβ intensity 17% larger than that given in Table 1 to account for self-absorption. The reasons for this correction were discussed by Ferland (1978).

b) The [O III] *Line Ratio*

Figure 4 shows the evolution of $R = I(5007, 4959)/I(4363)$, the familiar nebular to auroral line ratio.

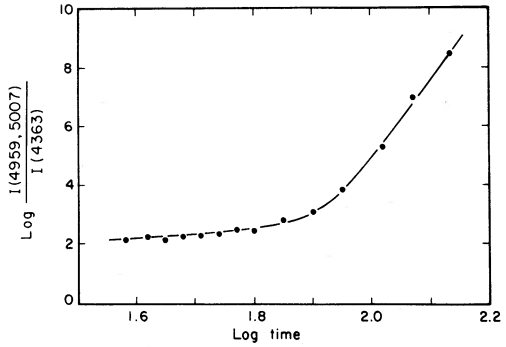

FIG. 4.—$I(5007, 4959)/I(4363)$. This ratio has been corrected for interstellar reddening and blending with Hγ as described in the text. The initial plateau shows that both ^1S and ^1D of O^{++} were thermalized until day 50. The ratio then increases as the population of ^1S falls because of the decreasing electron density.

The auroral line, λ4363, is blended with Hγ (λ4340), because of the large expansion velocity. We have removed the λ4340 contribution to the blend by estimating its strength from the strength of Hβ and Hδ and, alternatively, by fitting the blended line profile as shown in Figure 5. The deconvolution is accurate since λ4363 dominates the blend.

Figure 4 shows that R was nearly constant until day 50, when it began to increase because of the decreasing electron density. If the spontaneous emission probability from level 2, A_{21}, is much less than the collisional deexcitation rate, $N_e q_{21}$, then the population of level 2 will be determined by collisions and LTE may be assumed. The volume emission rate will be linear in density. When the critical density, $N_c \approx A_{21}/q_{21}$, is reached, both collisional and radiative deexcitation are important, and the balance equation

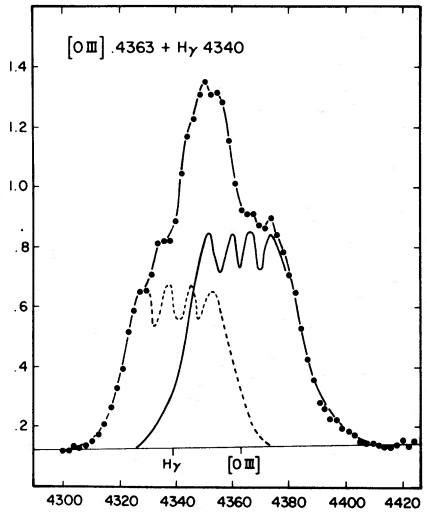

FIG. 5.—Hγ λ4363. The contribution of λ4363 to the blend has been estimated both by predicting the strength of Hγ from observations of Hβ and Hδ, and by fitting the outer wings of the line profile with lines similar to Hβ. This scan was obtained on day 40, when Hγ made its strongest contribution to the blend.

must be solved to determine the level population. At low densities, $A_{21} \gg N_e q_{21}$, and the emission rate equals the excitation rate. The volume emission rate will have a density-squared dependence. The plateau in Figure 4 suggests that both ^1S and ^1D were nearly thermalized until day 50. When the density fell to $N_e \approx 10^{7.5}$ cm^{-3}, ^1S could no longer be maintained in LTE, so its population fell more rapidly than that of ^1D (which remains in LTE until $N_e \approx 10^{5.8}$ cm^{-3}), causing R to increase.

R is related to the physical conditions of the O^{++} Strömgren sphere by the expression (Seaton 1975)

$$R = 7.2 \exp(3.30/t)\left(\frac{1 + 0.00054x}{1 + 0.063x}\right), \quad (1)$$

where $t = T_e/10^4$ K and $x = t^{-1/2}N_e/10^4$ cm^{-3}. The plateau before day 50 corresponds to $T_e \approx 9500$ K.

c) *The* [Ne III]/[O III] *Ratio*

The ratio of [O III] λλ5007, 4959 to [Ne III] λ3869 (Fig. 6) depends upon both density and temperature since the ^1D level of [Ne III] is thermalized at higher densities ($10^{6.6}$ cm^{-3}) than is that of [O III], and the excitation potentials differ. The neon line was blended with H8 and He I λ3888 until day 40, when λ3869 became the dominant contributor since λ3869/λ3968 has the correct (3:1) doublet ratio. The plateau in Figure 6 from day 40 to day 64 shows that the ^1D level of both ions was thermalized. The ratio decreases after day 64 since the density approaches the critical density for thermalization of ^1D of [Ne III]. Photoionization models show that the ionization fraction $N(O^{++})/N(Ne^{++})$ is constant since the two Strömgren spheres are nearly coincident. Seaton's (1975) results allow us to relate the ratio to the physical conditions and the O^{++}/Ne^{++} abundance ratio by

$$\frac{I(4959, 5007)}{I(3869)} = 1.83 \frac{N(O^{++})}{N(Ne^{++})} e^{0.423/t}\left(\frac{1 + 5.37 \times 10^{-4}x}{1 + 6.68 \times 10^{-5}x}\right) \times \frac{(1 + 1.11 \times 10^{-3}x + 6.95 \times 10^{-8}x^2)}{(1 + 1.79 \times 10^{-2}x + 9.37 \times 10^{-6}x^2)}. \quad (2)$$

d) *The* [O III]/He I *5876 Ratio*

The final temperature-density indicator is

$$I(5007, 4959)/\text{He I } \lambda 5876,$$

shown in Figure 7. The ratio will be inversely proportional to density since ^1D of O^{++} is thermalized, and λ5876 is an optically thin recombination line. It is also temperature-dependent through both the Boltzman factor for ^1D and the effective recombination coefficient of λ5876. The relative ionization fraction O^{++}/He^+ does not change since the O^{++} and He^+

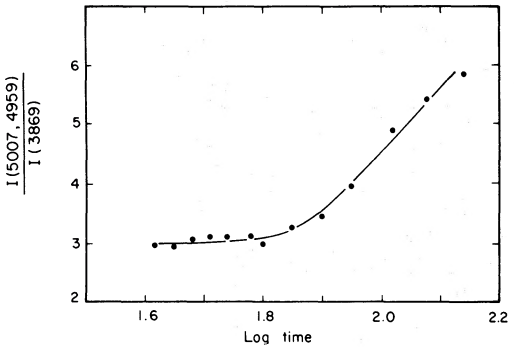

FIG. 6.—$I(5007, 4959)/I(3869)$. This is the [O III]/[Ne III] ratio before correcting for interstellar reddening. The plateau shows that ^1D of both ions was thermalized until day 67.

regions presumably are nearly coincident. Seaton's (1975) formulae give

$$\frac{I(4959, 5007)}{I(5876)} = 5.38 \times 10^9 \frac{N(O^{++})}{N(He^+)} \times \frac{xe^{-2.90/t}(1 + 5.37 \times 10^{-4}x)}{N_e(1 + 1.79 \times 10^{-2}x + 9.37 \times 10^{-6}x^2)}. \quad (3)$$

e) Results

This section combines the three density-temperature indicators, $I(5007, 4959)/I(4363)$, $I(5007, 4959)/I(5876)$, and $I(5007, 4959)/I(3869)$ to estimate the physical conditions within the ejecta at several epochs during the nebular phase. The three equations (1), (2), and (3) may be solved simultaneously. Observations at each epoch produce three data (the three line ratios), but, in general, introduce four unknowns (O^{++}/He^+, O^{++}/Ne^{++}, N_e, T_e). Photoionization models show that the O^{++}/He^+ and O^{++}/Ne^{++} abundance ratios

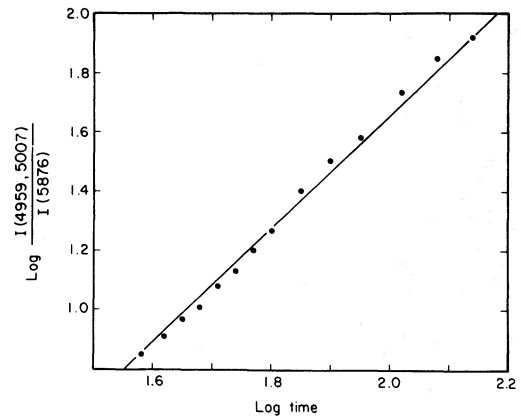

FIG. 7.—$I(5007, 4959)/I(5876)$. The plotted [O III]/He I ratio has not been corrected for interstellar reddening. The ratio has a nearly power-law time dependence since ^1D of O^{++} is thermalized throughout our observations, while λ5876 is an optically thin recombination line.

are independent of the physical conditions over a wide range of the parameters, so we introduce the approximation that they are independent of time. We are left with two unknowns per observation (N_e and T_e), and two (time-independent) variables, the abundance ratios. The data set comprises a system of $3N$ equations (where N is the number of observations), with $2N + 2$ unknowns, and can be solved with standard multiple nonlinear regression techniques. To our knowledge, this method has not been used before to derive abundances and physical conditions from nebular emission lines. The success of the method relies on the fact that the adopted line ratios have different dependences on N_e and T_e.

The results are summarized in Figure 8, which shows the run of density and temperature with time. The optimum values of the abundance ratios were $O^{++}/Ne^{++} = 6.9 \pm 0.4$ and $O^{++}/He^+ = 0.130 \pm 0.01$. The self-consistency of the procedure can be checked by computing all observed line ratios using these ionic abundances and the N_e, T_e values at each epoch. The predicted line ratios were usually within 3% of the observed values, and always within 5%. The error bars in Figure 8 were estimated by changing the line ratios to account for the uncertainty in the interstellar reddening.

f) The Need for a Continuing Energy Source

The H^+ recombination time scales, $\tau_{rec} = (N_e\alpha_B)^{-1}$, where α_B is the case B recombination coefficient, were (0.28, 0.98, and 5.0) days when the ejecta had ages of (41, 79, and 121) days. Because τ_{rec} is always much shorter than the time elapsed since outburst, the gas would have recombined if there were no continuing source of heat and ionization. We shall assume that photoionization is the only important energy source for the regions of the ejecta emitting the nebular lines (except for [Ne V] and [Fe VII]). Coronal emission lines were present after day 30 (Grasdalen and Joyce 1976; Fehrenbach and Andrillat 1976), but they were weak during the period that we are considering. The coronal conditions estimated by Ferland, Lambert, and Woodman (1977) indicate that the coronal line region does not make any significant contribution to the heating of the nebular line region.

g) The [Ne V] Region

The previous section derived the density and temperature of the nebular line region. These quantities are averages over the line-producing region, within which small fluctuations probably exist. The purpose of this section is to show that the nebular line region is fairly homogeneous, but that a second region, characterized by a much higher temperature, must also exist. This second region is the successor to the coronal line region detected earlier in the decline.

Because the expansion velocities are large in novae, it is possible to resolve the ejecta into components with the Doppler shift, even though the shell itself is not spatially resolved (see, e.g., Weaver 1974; Soderblum 1976). Emission lines generally have several

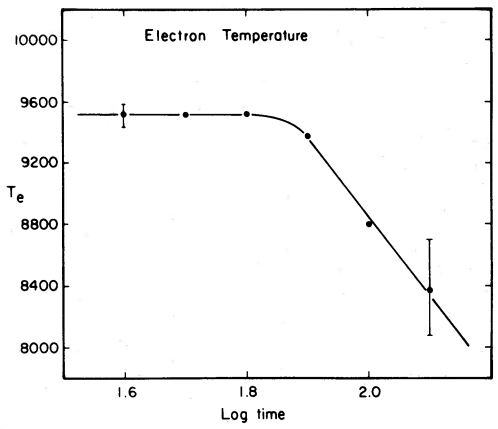

FIG. 8*a*

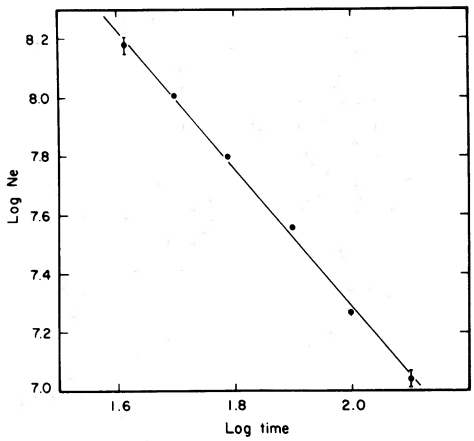

FIG. 8*b*

FIG. 8.—Measured density and temperature. These are the results of the simultaneous solution of the three line ratios. Error bars are due to uncertainties in the interstellar reddening.

components distributed symmetrically about the rest wavelength of the line. Hutchings (1972; also Hutchings and McCall 1977) has shown that this is almost certainly a geometrical effect; the ejecta often take the form of an equatorial ring (which Sparks and Starrfield 1972 identify as the remnant of the accretion disk) and a pair of polar blobs.

The analysis of the line intensities is sometimes complicated because these two regions sometimes have very different densities; they differed by roughly an order of magnitude in the very slow Nova HR Delphini 1967 (Gallagher and Anderson 1976). This caused the profiles of lines of various ionization potentials to differ since the physical conditions of the various line-producing regions differed (see Fig. 2 of Gallagher and Anderson 1976).

Consideration of the line profiles of Nova Cygni suggests that the physical conditions in the various components of the nebular line region do not differ by much. Figure 9, which is a detail from Figure 2, shows profiles of Hα, He I λ5876, and [O I] λ6300. The hydrogen line is formed throughout the ejecta, but the helium line is formed only within the He^+ Strömgren sphere. The [O I] line is formed within regions which are largely neutral since the ionization of O^0 and the ionization of H^0 are strongly coupled by charge exchange. (Hα is depressed on the approaching wing because of radiative transfer effects [Ferland 1978].)

The line profiles are all quite similar when due allowance is made for the depression of the blue wing of Hα. Slight differences are present (e.g., the inner components of λ6300 are weaker relative to the outer than are those of Hα or λ5876); but large-scale inhomogeneities, such as those in the ejecta from HR Del, cannot be present. This assertion is also supported by the close agreement between predicted and observed line ratios described in § III*e*.

A second line-producing region must also exist, however. Strong lines of [Ne V] were present during the late nebular stage. Photoionization models show that the He^{++} Strömgren sphere contains both Ne^{+3} and Ne^{+4}, but that the He^+ sphere contains almost entirely Ne^{++}. If we assume roughly the same physical conditions for the [Ne V] zone as we have derived for the [Ne III] zone, then the required [Ne V]/[Ne III] ratio exceeds the upper limit by a factor of 10 (even if Ne^{+4} is assumed to fill the entire He^{++} zone).

We propose that the [Ne V] emission originates within the coronal line region. Ferland, Lambert, and Woodman (1977) traced the evolution of Nova Cygni's coronal line spectrum during the first year of the outburst. Both [Fe X] λ6374 and [Fe XI] λ7892 were first detected above the strong continuum on day 30. Their relative strengths implied $T_e \approx 10^{6.1}$ K, which fell as the nova aged. The subcoronal line [Fe VII] λ6087 was first detected on day ~50, when the temperature had fallen to $10^{5.7}$ K. The strength of λ6087 increased (relative to the coronal lines) as the temperature approached $10^{5.4}$ K, where Fe^{+6} is the dominant stage of ionization (Jordan 1969).

The ionization potentials of Ne^{+4} and Fe^{+6} are fairly similar (Nussbaumer and Osterbrock 1970), so the fractional abundance of Ne^{+4} within the coronal line region will be large when Fe^{+6} is prominent. The mass fraction within the coronal line region may be estimated from the relative [Ne V]/[Ne III] ratio if we assume that λ3426 originates entirely within the coronal line region with $T_e \approx 10^{5.4}$ K, that λ3869 is produced in the nebular line region ($T_e = 8500$ K), and that ^1D of both ions is thermalized. Then $I(3426)/I(3869) = 1.4$ corresponds to $N(Ne^{+4})/N(Ne^{++}) = 0.02$. Only a modest fraction of the mass of the ejecta is in the coronal line region, in agreement with previous estimates.

IV. THE CHEMICAL ABUNDANCES

a) Oxygen

Three stages of ionization (O^0, O^+, and O^{++}) are observed, and their abundances can be measured

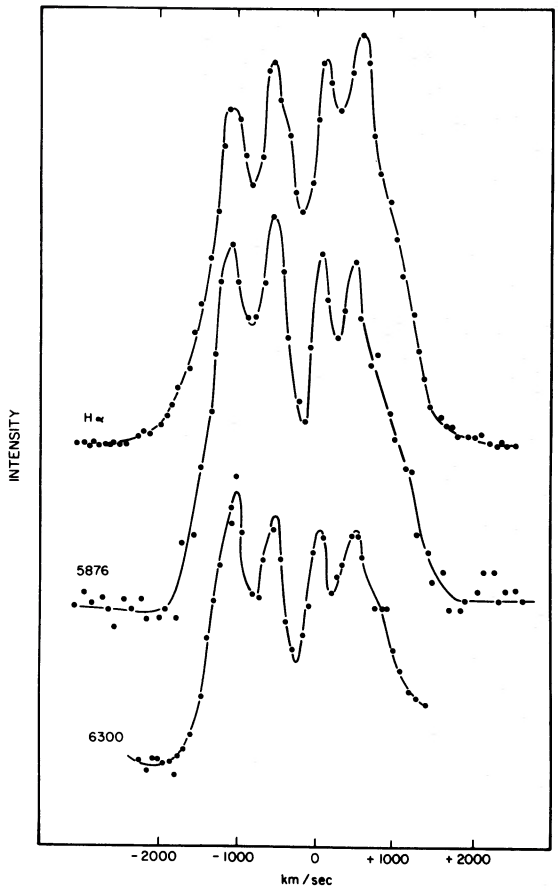

FIG. 9.—Line profiles. The profiles of [O I] λ6300, He I λ5876, and Hα are compared. Hα is depressed on the blue wing because of self-absorption. The red wing of [O I] λ6300 is blended with [O I] λ6363. The profiles are fairly similar, showing that the emitting regions have similar densities.

directly. The ionization potentials of O^{++} and He^{+} are similar (Moore 1970), so we make the common assumption that O^{+3} and higher stages of ionization exist only within the He^{++} Strömgren sphere. Then

$$\frac{N(O^{+}, O^{++})}{N(O)} = \frac{N(He^{+})}{N(He^{+}) + N(He^{++})}. \quad (4)$$

We shall assume that the physical conditions within the O^{++} zone also apply to the O^{+} region. This approximation is not critical since only a small fraction of the oxygen is in the form of O^{+}.

The emissivity per ion for [O III] λλ5007, 4959 was taken from Seaton (1975). The emissivity of the [O II] λ7325 blend and [O I] λ6300 was derived from the solution of the five-level atom with the atomic constants collected by Osterbrock (1974); and the He^{++}/He^{+} ratio was taken from Ferland (1978). The results are summarized in Table 2. The $(O^{+} + O^{++})/H^{+}$ ratio decreases during the interval, but the total O/H ratio (0.0165) is constant. Systematic errors (e.g., atomic constants, the correction for interstellar reddening) make this uncertain to 0.1 dex.

b) Neon

Photoionization models show that, within 10%, $N(Ne^{++})/N(Ne) = N(O^{++})/N(O)$ over a wide range of physical conditions. The O^{++}/Ne^{++} ratio (6.9 ± 0.4) is a by-product of our analysis of the physical conditions in § III. The neon abundance is Ne/H = 0.0024 ± 0.0006.

c) Nitrogen

No calibrated recombination lines are available. The strong N III λ4640 multiplet is probably formed by either continuum fluorescence (Gallagher 1978) or the Bowen mechanism (Bowen 1947). Strong [N II] λλ6548, 6584 was present when the nova was much older ($t \approx 300$ days), but the auroral [N II] λ5755 was present throughout the nebular phase. The N^{+}/O^{+} ratio may be measured directly by comparing the strengths of the two auroral lines, λ5755 and λ7325.

Figure 10 shows lines of constant $\epsilon(7325)/\epsilon(5755)$ on the $\log(N_e)$-T_e plane. The emission lines have similar collision strengths and excitation potentials, so the predicted line ratio is insensitive to the physical conditions. The path of the nova is marked in the figure.

On day 40, λ5755 is blended with several [Fe II] and Fe II lines, but by day 80, λ5755 is the dominant contributor, since the line's castellated structure is clear. The mean of four observations between days 80 and 120 is $I(5755)/I(7325) = 1.18 \pm 0.05$ (standard deviation), after correcting for interstellar reddening. The relative ionic abundance becomes $N(N^{+})/N(O^{+}) = 0.71 \pm 0.10$. Photoionization models show that $N(N^{+})/N(N) \approx N(O^{+})/N(O)$, within ~0.1 dex, so the total nitrogen abundance is N/H = 0.011 ± 0.2 dex.

d) Iron

The Ne/Fe ratio may be obtained from [Ne V] λ3426/[Fe VII] λ6087 since $N(Ne^{+4})/N(Ne) \approx N(Fe^{+6})/N(Fe)$, because both ions have similar ionization potentials (Nussbaumer and Osterbrock 1970).

TABLE 2

OXYGEN ABUNDANCE OF NOVA CYGNI*

t_{days}	O^{0}/H^{+}	O^{+}/H^{+}	O^{++}/H^{+}	He^{++}/He^{+}	O/H
42.....	0.0016	0.0008	0.0139	0.13	0.0166
79.....	0.0007	0.0008	0.0128	0.20	0.0163
121.....	0.0002	0.0014	0.0120	0.28	0.0171

* By number of atoms.

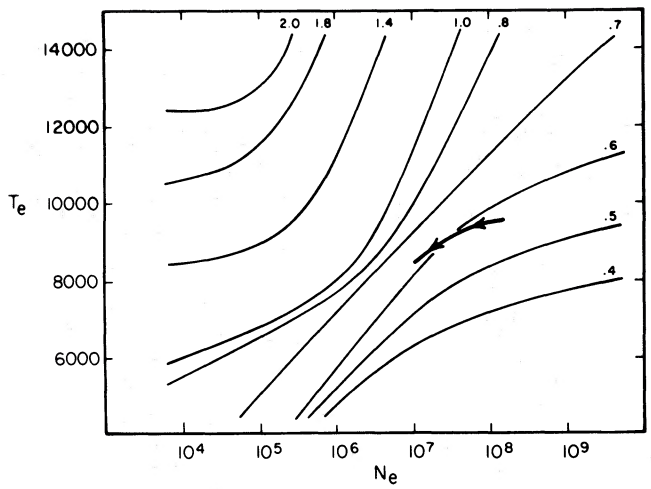

FIG. 10.—$j(7325)/j(5755)$. This figure shows the ratio of the unit emissivity of the [O II] λ7325 blend to that of [N II] λ5755, as a function of both electron temperature and density. The path of the nova is marked.

Section III has shown that these lines originate within the shock-ionized coronal line region. Jordan (1969) has computed ionization corrections, $\log [N(A^i)/N(A)]$ for steady-state collisional ionization. The strength of λ6087, relative to the other coronal lines, peaked on day 140 (Ferland, Lambert, and Woodman 1977). This determines the temperature since the line will be strongest when Fe^{+6} is the dominant stage of ionization. Jordan's (1969) calculations show that $\log (T_e) = 5.3 \pm 0.1$ and $\log (Ne^{+4}/Ne) - \log (Fe^{+6}/Fe) = -0.4 \pm 0.4$. The error is due to the uncertainty in T_e.

The level 2 populations of both Ne^{+4} and Fe^{+6} have been solved assuming a five-level atom and steady state. The atomic parameters are from Garstang (1968), Saraph, Seaton, and Shemming (1969), and Nussbaumer and Osterbrock (1970). Figure 11 shows the ratio of emissivities per ion $\epsilon(3426)/\epsilon(6087)$ as a function of N_e and T_e. The electron density in the coronal line region is poorly known; but it is evidently safe to assume $\epsilon(3426)/\epsilon(6087) \approx 1.5 \pm 0.2$, since the ratio is fairly insensitive. For this value and the above ionization correction, we have $N(Ne)/N(Fe) \approx 1.7\, I(3426)/I(6087)$. The average of three observations centered about day 140 is $I(3426)/I(6087) = 45 \pm 5$. The model calculations described later were used to make a small correction (~20%) to the line strengths to account for emission originating within the nebular line region. The final abundance ratio is $N(Fe)/N(Ne) = 0.013$ or $Fe/H = 3 \times 10^{-5}$, uncertain to 0.5 dex because of the ionization correction. This iron abundance is close to the solar value 2.6×10^{-5} (Cameron 1973). (The derived iron abundance would be essentially the same if the [Fe VII] and [Ne V] emission were assumed to come from photoionized gas with the same physical conditions as in the [O III] zone.)

e) Carbon

Permitted lines of C II (λ4267) and C III (λ4187) are observed in Nova Cygni. Grandi (1976) has shown that these lines are formed mainly by recombination, so they may be compared directly with Balmer lines to measure the C^{+2} and C^{+++} abundances.

The strongest C II line, λ4267, is unblended since it shows the castellated structure common to the emission lines of Nova Cygni. Figure 12 shows the observed ratio $I(4267)/I(H\beta)$. The constancy of this ratio supports the assumption that the line results from recombination, since fluorescent emission presumably would have varied as the stellar continuum evolved. The straight mean is $I(4267)/I(H\beta) = 0.040 \pm 0.008$, after correcting for interstellar reddening. The C^{+2} abundance was computed from the formula $C^{+2}/H^+ = 0.13\, I(4267)/I(H\beta)$, which is based on an expression by Aller (1977) based on recombination coefficients by Bednarek and Clarke. This is in excellent (10%) agreement with the expression derived from the

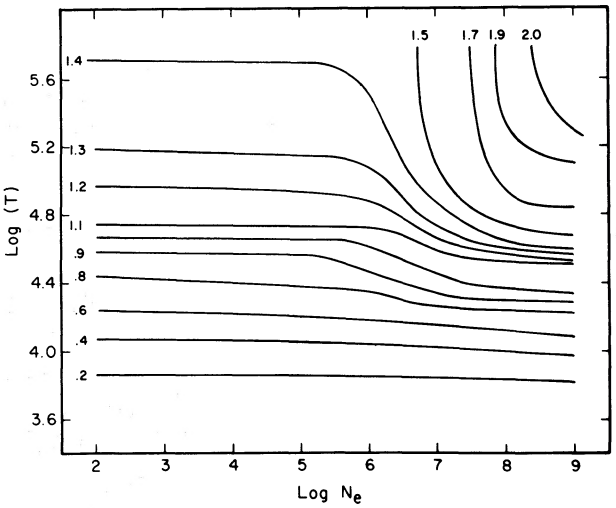

FIG. 11.—$j(3426)/j(6087)$. [Ne V]/[Fe VII] emissivity ratio analogous to Fig. 10.

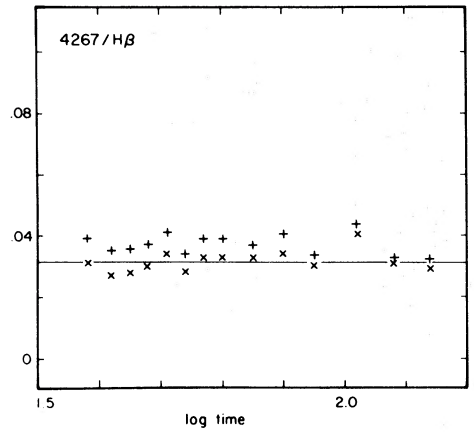

FIG. 12.—$I(4267)/I(H\beta)$. This figure shows the strength of C II λ4267 as a function of time. The upper points are the observed ratios, while the lower set have been corrected for Hβ self-absorption.

effective recombination coefficient $\alpha_{\rm eff}(\lambda 4267) = 2.5 \times 10^{-13}$ cm^3 s^{-1} at 10^4 K given by Pengelly (1963) and $\alpha_{\rm eff}(H\beta)$ given by Brocklehurst (1971). The result is $N(C^{++})/N(H^+) = 0.005 \pm 0.001$.

The strongest C III lines, λλ4647, 4650, and 4651, lie within the broad blend of lines dominated by N III 4640 and He II 4686. The next strongest line, λ4070, is present in the blue wing of Hβ; but [S II] λλ4067, 4076 and several N II lines may also contribute to its strength. The λ4187 line is apparently unblended. Figure 13 shows the strength of this line relative to Hβ. The ratio is uncertain since λ4187 is very weak No significant trend with time is present. For the C^{+3} abundance, we started with the expression $C^{+3}/H^+ = 0.18\ I(4647, 4650, 4651)/I(H\beta)$ given by Shields (1978*a*) on the basis of an expression by Aller (1977). To derive the corresponding expression for λ4187, we used the ratio $I(4187)/I(4647, 4650, 4651)$ observed for NGC 7027 by Kaler *et al.* (1976). This gives $C^{+3}/H^+ \approx 0.5\ I(4187)/I(H\beta)$. For Nova Cygni, we thus have $C^{+3}/H^+ = 0.007$. The systematic error

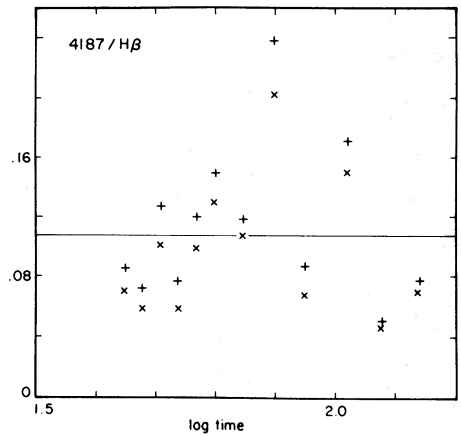

FIG. 13.—$I(4187)/I(H\beta)$. The strength of C III λ4187, presented as in Fig. 12.

introduced by the scaling procedure is difficult to estimate, and it could be a factor 2 or 3.

Photoionization models show that nearly all the carbon will be either doubly or triply ionized, so only a slight (10%) correction must be made to obtain the total carbon abundance (C/H = 0.013 ± 0.004). We note that the C^{+2} abundance alone is an order of magnitude larger than the solar carbon abundance. Model calculations described below provide independent confirmation of the derived carbon abundance.

f) *Sulfur*

The absence of [S III] λλ9069, 9532 emission lines sets an upper limit to the sulfur abundance of the ejecta. The S^{+2}/O^+ ratio can be predicted accurately (after making a small correction for the slightly different ionization fractions) since doubly ionized sulfur should be present mainly in the O^+ zone.

The strongest sulfur line should be λ9532, which is blended with P8 λ9546. The Paschen decrement appears normal, so the sulfur line can contribute less than half the flux in the Paschen line. The reddening-corrected upper limit is

$$\frac{I([\text{S III}]\ 9532)}{I([\text{O II}]\ 7325)} < 0.1\,,$$

and comparison with model calculations (see below) sets the limit

$$\frac{N(\text{S})}{N(\text{O})} < 0.004\,,$$

or $N(S)/N(H) < 6 \times 10^{-5}$. The abundance of sulfur is less than 4 times the solar abundance.

V. MODEL CALCULATIONS

This section compares the line intensities and physical conditions described above with theoretical predictions from model nebulae. Details of the program have been described elsewhere (Shields 1978*a*). Briefly, it includes the effects of H, He, C, N, O, Ne, Fe, S, and Mg on the ionization structure and thermal equilibrium of a steady-state photoionized nebula. No attempt will be made to model the conditions within the coronal line region, and the effects of dust are neglected.

The steady-state assumption is reasonably good during the portion of the outburst that we consider here. The recombination time scale is always short compared with the rate of decline of the nova, so the ionization structure will be nearly steady-state. A quasi-periodic ($P \approx 3$ hr) "ripple" is superposed upon the smooth decline of the light curve (Tempesti 1975; Campbell 1976). The amplitude was small (~5%) on day 40 when $\tau_{\rm rec}$ was of order 3 hr, so the effects should also be small. Later, when the amplitude was larger (~20%), $\tau_{\rm rec}$ was much longer than 3 hr, so the variation will be averaged out by the gas. Ionization and thermal equilibrium is an acceptable approximation.

The first part of this section discusses the model parameters. The effects of the chemical abundances upon the thermal equilibrium are then discussed, followed by a comparison between the predicted and observed line intensities.

a) Model Parameters

In general, three quantities characterize a photoionization model: the shape of the ionizing radiation field, the chemical composition of the gas, and the ionization parameter $U = Q(\mathrm{H})/4\pi R^2 N_e c$, where $Q(\mathrm{H})$ is the ionizing photon luminosity (s^{-1}) of the central star and R is the radius of the ejecta. The chemical composition and electron density were taken from previous sections of this paper.

The radius of the ejecta is determined by the expansion velocity and the elapsed time from outburst. The slope of the rising branch of the infrared light curve suggests that the expansion started at 1975 August 28.5 (Gallagher and Ney 1976; Ennis *et al.* 1977; Barnes 1976). The expansion velocity is uncertain, but optical data suggest $\sim 10^3$ km s^{-1} (Tomkin, Woodman, and Lambert 1976). This may be uncertain by as much as 0.3 dex.

A blackbody ionizing radiation field was assumed. The color temperature was adjusted to produce the observed $\mathrm{He}^{++}/\mathrm{He}^{+}$ ratio. This is determined by

$$\frac{Q(\mathrm{He}^{++})}{Q(\mathrm{He}^{+})} = \frac{\int_4^\infty F_\nu/h\nu d\nu}{\int_{1.8}^4 F_\nu/h\nu d\nu}, \qquad (5)$$

since the helium abundance is so large that it dominates the radiative transfer of photons with energies greater than 1.8 rydberg (Hummer and Seaton 1964; Harmon and Seaton 1966).

The total ionizing flux can be estimated from the recombination rate if we can estimate the optical depth of the ejecta to ionizing photons, and the covering factor, i.e., the fraction of a sphere covered by the ejecta. The recombination rate was estimated from the power in Hβ, assuming a distance of 1800 pc and a color excess of $E(B-V) = 0.51$ (Ferland 1977).

The ejecta are likely to be optically thick to ionizing photons since neutral oxygen emission was observed throughout the decline. The covering factor is unknown since the ejecta have not been spatially resolved. Photographs of ejecta from other novae (Mustel and Boyarchuk 1972) suggest that the covering factor, $\Omega/4\pi$, is likely to be within 1 dex of 0.1. The ionizing flux is uncertain to this amount since $Q(\mathrm{H}) \propto L(\mathrm{H}\beta)/\Omega$. The adopted values of $Q(\mathrm{H})$, based on $\Omega/4\pi = 0.10$, are listed in Table 3.

Models were computed with conditions estimated for each of the three epochs tabulated in Table 1. A synopsis of the model parameters and the results are listed in Table 3. The line intensities for day 42 should be multiplied by 1.17 before comparison with Table 1, to allow for Hβ self-absorption.

b) Thermal Equilibrium and Line Intensities

The electron temperatures during the nebular phase of Nova Cygni (Fig. 8) are low by nebular standards.

TABLE 3

RESULTS OF MODEL CALCULATIONS

t_{days}	42	79	121
Model Parameters			
R^* (cm)	3.5×10^{14}	6.9×10^{14}	1.0×10^{15}
$Q(\mathrm{H})$ (s^{-1})	1.5×10^{49}	3.3×10^{48}	9.5×10^{47}
T_{bb} (K)	110000	120000	130000
N_e (cm^{-3})	1.5×10^{8}	3.3×10^{7}	1.2×10^{7}
$T(\mathrm{O}^{++})$ (K)†	9300	9000	8700
Line Intensities			
Hβ λ4861	1.00	1.00	1.00
[O I] λ6300	0.0001	0.001	0.008
[O II] λ7325	0.0006	0.0056	0.025
[O III] $\lambda\lambda$5007, 4959	1.51	6.03	13.4
[O III] λ4363	0.64	1.68	2.17
[Ne III] λ3869	0.85	2.78	4.57
[Ne V] λ3426	0.048	0.163	0.64
C III] λ1909	21.2	16.2	11.1
C IV λ1550	5.1	4.5	7.2
N III] λ1750	2.67	2.00	1.37
N IV λ1486	1.5	1.3	1.3

* Inner radius of shell.

† Computed equilibrium temperature.

This is because the large overabundances of some elements provide an efficient coolant for the gas so that thermal equilibrium is attained at lower kinetic temperatures.

Table 3 lists the model predictions for the temperature of the O^{++} Strömgren sphere. These match the observed T_e fairly well. Table 3 also lists the predicted strengths of some strong ultraviolet lines which are significant coolants. Two carbon lines, C III] λ1909 and C IV λ1550, dominate the emission line cooling.

Table 4 explores the effects that changes of the heavy-element abundances have on T_e. It also lists O^{++} electron temperatures at various carbon abundances and, in the last column, for a solar mixture. A large carbon abundance (C/H $\approx$ 0.01) is required to reproduce the electron temperature of the ejecta. This confirms the result derived above from the recombination lines.

The predicted nebular line strengths (Table 3) are in mixed agreement with observations. Both [Ne V] λ3426 and [Fe VII] λ6087 are underestimated since they are formed mainly in the coronal line region. The models also fail to predict the strength of lines from transition-zone ions such as [O II] λ7325, [N II] λ5755, and [O I] λ6300. This is a common problem with models of other photoionized objects (e.g., planetary nebulae and Seyfert galaxy nuclei) and may be due to nonequilibrium phenomena (Shields and Oke 1975).

Figure 14 shows the temperature and fractional abundances of several ions as a function of depth in the ejecta. An interesting feature is that the large metal abundances lead to a C^{+3} Strömgren sphere

TABLE 4

THERMAL EQUILIBRIUM IN MODELS

t_{days}	$T(O^{++})$ (K)*	C/H†					
		0.012	0.008	0.004	0.001	0.0005	All Solar
42.....	9500 ± 200	9300	9600	10000	10800	11000	12500
79.....	9300 ± 300	9000	9200	9600	10000	10400	12100
121.....	8400 ± 400	8700	8900	9200	9400	9600	11500

* Observed value.

† Abundances other than C were those of Table 5, except for "all solar" model.

well inside that of H^+, in contrast to the case for nebulae with solar abundances.

The ionization structure of oxygen is also interesting. Because of the high density, a significant fraction (~ 0.022) of O^{++} is in the ^1D state. Thus O^{++} can be destroyed in the He^+ zone by photons in the interval $3.86\nu_H$ to $4.00\nu_H$ (Burbidge and Burbidge 1967). The equilibrium equation is

$$\frac{N(O^{+3})}{N(O^{+2})} = \frac{N(^1D)}{N(O^{+2})} \frac{\Gamma(^1D)}{\alpha_B(O^{+3})N_e}, \quad (6)$$

where $\Gamma = a\nu\Delta\phi$ is the photoionization rate, $a_\nu = 4 \times 10^{-18}$ cm^2 (Henry 1970), $\alpha_B = 3.2 \times 10^{-12}$ cm^3 s^{-1} at 10^4 K (Aldrovandi and Pecquinot 1973), and $\Delta\phi$ is the photon flux (cm^{-2} s^{-1}) between 3.86 and $4.00\nu_H$. With $y \equiv \Delta\phi/\phi$ and $\phi = Q(H)/4\pi R^2$, this gives

$$\frac{N(O^{+3})}{N(O^{+2})} = 10^{2.9} yU. \quad (7)$$

For the assumed blackbody continuum (140,000 K), $Y = 0.017$. From Table 3, we find that U decreased from $10^{0.3}$ on day 42 to $10^{-0.7}$ on day 121, so that there should have been very little O^{++} in the nebula, according to equation (7). In fact, O^{++} is abundant because the photons between $3.86\nu_H$ and $4.00\nu_H$ are exhausted in a thin shell outside the He^{++} Strömgren sphere, whose relative volume is

$$\frac{V(O^{+3})}{V(H^+)} \approx Y \frac{\alpha_B(H^0)}{\alpha_{13}(O^{+2})} \frac{N(H)}{N(O)}. \quad (8)$$

For $Y = 0.017$ and $N(O)/N(H) = 10^{-1.8}$, this gives $V(O^{+3})/V(H^+) = 0.09$, and O^{++} fills most of the He^+ zone. Without the high metal abundances, O^{+3} might fill most of the He^+ zone.

VI. MASS OF THE EJECTA

The ionized portion of the mass is related to the Hβ luminosity through the expression

$$M_i \approx 2.05 m_H \frac{L(H\beta)}{\alpha_{42}^{eff} h\nu N_e}, \quad (9)$$

where $\alpha_{42}^{eff} h\nu = 1.24 \times 10^{-25} t^{-0.9}$ ergs cm^3 s^{-1} (Brocklehurst 1971) and the composition in Table 5 is assumed. This is a lower limit to the mass since neutral hydrogen must be present (O^0 is present). The ionized mass fell from 1.3×10^{29} g on day 40 to 8.5×10^{28} g by day 120. The mass decreases if the ionizing photon flux falls faster than the electron density, since the three are related (in steady state) by $Q(H^0) \propto N_e N_p V \propto N_e M_i$. This lower limit is similar to the ionized mass of Nova HR Delphini 1976 ($\sim 1.8 \times 10^{29}$ g) in 1975 (Anderson and Gallagher 1977). A similar trend toward smaller mass at later time may have been present there too, since Malakpur (1973) found the mass to be 40% larger during the early nebular stage.

VII. RESULTS AND DISCUSSION

We have measured the abundances of C, N, O, Ne, and Fe in the ejecta from the very fast Nova V1500 Cygni. Unlike previous analyses, we have modeled the evolution of the nova from the beginning of the nebular phase, when recombination lines dominated the spectrum, through its evolution into a typical old nova spectrum, dominated by forbidden line emission. The parameters derived in the analysis are in very good agreement with model calculations. The chemical abundances, together with solar abundances (Lambert 1978; Cameron 1973) are listed in Table 5.

C, N, O, and Ne are strongly overabundant. We suggest that the great strength of O I λ8446 (Strittmatter *et al.* 1977) is partly attributable to the high oxygen abundance, in addition to Lβ pumping com-

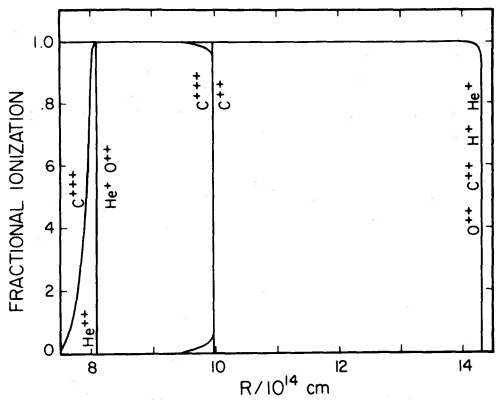

FIG. 14.—Fractional ionic abundances as a function of radius in the photoionization model for day 81.

TABLE 5

CHEMICAL ABUNDANCES OF V1500 CYGNI*

	V1500 Cygni	Sun	Nova − Sun
He/H.....	−0.96 ± 0.04	−0.96	0.0
C/H.....	−1.92 ± 0.1	−3.33	+1.4 ± 0.2
N/H.....	−1.96 ± 0.2	−4.00	+2.0 ± 0.2
O/H.....	−1.78 ± 0.1	−3.08	+1.3 ± 0.1
Ne/H.....	−2.62 ± 0.2	−3.96	+1.3 ± 0.2
Fe/H.....	−4.52 ± 0.3	−4.59	+0.1 ± 0.3

* Log $N(\mathrm{Ar})/N(\mathrm{H})$.

Solar system values from Lambert 1978 and Cameron 1973.

bined with Balmer self-absorption (Shields 1974). [It is interesting that $I(8446)/I(\mathrm{H}\alpha)$ had a maximum value 0.3, compared with a typical value ~ 0.05 in Seyfert galaxies (Oke and Shields 1976). Thus $\lambda 8446$ was stronger in the nova by roughly the magnitude of the oxygen overabundance.]

The large abundances also affect the thermal equilibrium of the gas since the additional ions provide an efficient coolant for the gas. The kinetic temperatures are always much lower ($T_e \approx 9000$ K) than those found in planetary nebulae of similar ionization ($T_e \approx 13{,}000$ K).

Both the iron and helium abundances are solar. The low iron abundance may reflect the intrinsic abundance of ejecta, but it could also be affected by depletion onto grains (Shields 1978*a*, *b*). The cosmic helium abundance is a characteristic V1500 Cygni shares with many other novae (Ferland, in preparation). Evidently, the source of the large C, N, O, and Ne abundances has little affect on the helium content of the ejecta. This is consistent with Colvin *et al.*'s (1977) suggestion that the chemical enhancements are the result of convective mixing of the outer layers of the white dwarf with its carbon core. The large abundances of C, O, and Ne presumably come from the white dwarf, whereas the abundance ratios He/H and Fe/H are those of the companion star that originally transferred the ejected material onto the white dwarf. The large abundance of nitrogen may result from proton capture during the thermonuclear runaway.

The large neon excess is confirmed by the identification of strong [Ne II] 12.8 μm emission from Nova Cygni (Ferland and Shields 1978). A thermonuclear runaway initiating the nova outburst seems unlikely to manufacture the excess neon (Truran 1978), and therefore the white dwarf itself may be largely composed of neon in addition to carbon and oxygen.

Robbins and Sanyal (1978) found that ejecta from the very slow Nova HR Delphini (1967) had a solar oxygen abundance, whereas we have found large enhancements in the very fast Nova V1500 Cygni. These results support Sparks, Starrfield, and Truran's (1978) suggestion that nova speed classes are determined by the chemical composition of the ejecta. Since the CNO nuclei act as a catalyst, novae with larger abundances should have greater peak luminosities and more rapid expansion velocities than those with more nearly solar abundances. Careful analysis of intermediate-speed novae is needed.

Williams *et al.* (1978) have measured similarly large C, N, and O abundances in the nebula surrounding the old nova DQ Her (1934). Carbon recombination lines (and hence the carbon abundance) in DQ Her are ~ 7 times stronger than those in V1500 Cygni. (Numerical values of the carbon abundance cannot be compared directly because different values of the effective recombination coefficient are used.) The large overabundance of carbon in DQ Her is surprising in light of Sparks, Starrfield, and Truran's (1978) ideas, and because much of the carbon should have condensed onto grains.

We are deeply indebted to Professor D. L. Lambert for his invaluable advice and encouragement, and to Professor Harlan J. Smith for his enthusiastic support of the nova program.

REFERENCES

Aldrovandi, S. M., and Pecquinot, D. 1973, *Astr. Ap.*, **25**, 137.

Aller, L. H. 1977, personal communication.

Aller, L. H., and Liller, W. 1969, in *Nebulae and Interstellar Matter*, ed. B. M. Middlehurst and L. H. Aller (Chicago: University of Chicago Press).

Anderson, C., and Gallagher, J. S. 1977, *Pub. A.S.P.*, **89**, 264.

Audouze, J., Lequeux, J., and Vigroux, L. 1975, *Astr. Ap.*, **43**, 71.

Barnes, T. G. 1976, *M.N.R.A.S.*, **177**, 53P.

Bowen, I. 1947, *Pub. A.S.P.*, **59**, 196.

Brocklehurst, M. 1971, *M.N.R.A.S.*, **153**, 471.

Burbidge, G., and Burbidge, M. 1967, *Quasi-Stellar Objects* (San Francisco: Freeman).

Cameron, A. G. W. 1973, in *Explosive Nucleosynthesis*, ed. D. N. Schramm and W. D. Arnett (Austin: University of Texas Press).

Campbell, B. 1976, *Ap. J.* (*Letters*), **207**, L41.

Collin-Souffrin, G. 1977, *Novae and Related Stars*, ed. M. Friedjung (Dordrecht: Reidel), p. 123.

Colvin, J. D., van Horn, H. M., Starrfield, S. G., and Truran, J. W. 1977, *Ap. J.*, **212**, 791.

Ennis, D., Becklin, E., Beckwith, S., Elias, J., Gatley, I., Matthews, K., Neugebauer, G., and Willner, S. 1977, *Ap. J.*, **214**, 478.

Fehrenbach, Ch., and Andrillat, Y. 1976, *Astr. Ap.*, **52**, 123.

Ferland, G. J. 1977, *Ap. J.*, **215**, 873.

———. 1978, *Ap. J.*, **219**, 589.

Ferland, G. J., Lambert, D. L., and Woodman, J. 1977, *Ap. J.*, **213**, 132.

Ferland, G. J., and Shields, G. A. 1978, *Ap. J.* (*Letters*), **224**, L15.

Gallagher, J. S. 1978, preprint.

Gallagher, J. S., and Anderson, C. M. 1976, *Ap. J.*, **203**, 625.

Gallagher, J. S., and Ney, E. P. 1976, *Ap. J.* (*Letters*), **204**, L35.

Garstang, R. H. 1968, *IAU Symposium No. 34, Planetary Nebulae*, ed. D. E. Osterbrock and C. R. O'Dell (Dordrecht: Reidel), p. 143.

Grandi, S. 1976, *Ap. J.*, **206**, 658.

Grasdalen, G., and Joyce, R. R. 1976, *Nature*, **259**, 187.

Harmon, R., and Seaton, M. J. 1966, *M.N.R.A.S.*, **132**, 15.

Henry, R. J. W. 1970, *Ap. J.*, **161**, 1153.

Hummer, D., and Seaton, M. 1964, *M.N.R.A.S.*, **127**, 217.

Hutchings, J. B. 1972, *M.N.R.A.S.*, **158**, 177.
Hutchings, J. B., and McCall, M. 1977, *Ap. J.*, **217**, 775.
Jordan, C. 1969, *M.N.R.A.S.*, **142**, 501.
Kaler, J. B., Aller, L. H., Czyzak, S. J., and Epps, H. W. 1976, *Ap. J. Suppl.*, **31**, 163.
Lambert, D. L. 1978, *M.N.R.A.S.*, in press.
Malakpur, I. 1973, *Astr. Ap.*, **24**, 125.
McLaughlin, D. B. 1936, *Ap. J.*, **84**, 104.
Miller, J. S., and Mathews, W. G. 1972, *Ap. J.*, **172**, 593.
Moore, C. E. 1970, NSRDS–NBS 34.
Mustel, E. R., and Boyarchuk, A. A. 1972, *Ap. Space Sci.*, **6**, 183.
Nussbaumer, H., and Osterbrock, D. E. 1970, *Ap. J.*, **161**, 811.
Oke, J. B., and Shields, G. A. 1976, *Ap. J.*, **207**, 713.
Osterbrock, D. E. 1974, *Astrophysics of Gaseous Nebulae* (San Francisco: Freeman).
Payne-Gaposchkin, C. 1957, *The Galactic Novae* (New York: North-Holland).
Pengelly, R. M. 1963, Ph.D. thesis, University of London (kindly communicated by M. J. Seaton).
Pottasch, S. 1959, *Ann. d'Ap.*, **22**, 412.
Robbins, R. R., and Sanyal, A. 1978, *Ap. J.*, **219**, 985.
Saraph, H. E., Seaton, M. J., and Shemming, J. 1969, *Phil. Trans. Roy. Soc. London*, **264**, 77.
Seaton, M. J. 1975, *M.N.R.A.S.*, **170**, 4751.
Shields, G. A. 1974, *Ap. J.*, **191**, 309.
———. 1978*a*, *Ap. J.*, **219**, 559.
———. 1978*b*, *Ap. J.*, **219**, 565.
Shields, G. A., and Oke, J. B. 1975, *Ap. J.*, **197**, 5.
Sneden, C., and Lambert, D. L. 1975, *M.N.R.A.S.*, **170**, 533.
Soderblum, D. N. 1976, *Pub. A.S.P.*, **88**, 517.
Sparks, W., and Starrfield, S. G. 1973, *M.N.R.A.S.*, **164**, 1P.
Sparks, W., Starrfield, S., and Truran, J. 1978, *Ap. J.*, **220**, 1063.
Spencer-Jones, H. 1931, *Cape Obs. Ann.*, **10**, part 9.
Starrfield, S., Sparks, W. M., Warren, M., and Truran, J. 1974, *Ap. J. Suppl.*, **28**, 247.
Starrfield, S., Truran, J., Sparks, W., and Kutter, G. 1972, *Ap. J.*, **176**, 169.
Strittmatter, P., *et. al.* 1977, *Ap. J.*, **216**, 23.
Tempesti, P. 1975, *Inf. Bull. Var. Stars* No. 1052.
Tomkin, J., Woodman, J., and Lambert, D. L. 1976, *Astr. Ap.*, **48**, 319.
Truran, J. 1978, personal communication.
Weaver, H. 1974, in *Highlights of Astronomy*, **3**, 509.
Whitford, A. E. 1958, *A.J.*, **63**, 201.
Williams, R. E. 1977, in *IAU Colloq. No. 42*, in preparation.
Williams, R. E., Woolf, N., Hege, E., Moore, R., and Kopriva, D. 1978, *Ap. J.*, in press.
Young, P., Corwin, H., Bryan, J., and de Vaucouleurs, G. 1976, *Ap. J.*, **209**, 882.

GARY J. FERLAND: Institute of Astronomy, University of Cambridge, Cambridge CB3 0HA, England

GREGORY A. SHIELDS: University of Texas at Austin, Department of Astronomy, 15.212 R.L. Moore Hall, Austin, TX 78712